Aalborg Universitet

AALBORG UNIVERSITY

DENMARK

A Cost-Effective Power Ramp-Rate Control Strategy for Single-Phase Two-Stage Grid-Connected Photovoltaic Systems

Ariya Sangwongwanich[1], Yongheng Yang[2], *IEEE Member*, and Frede Blaabjerg[3], *IEEE Fellow*

Department of Energy Technology
Aalborg University
Pontoppidanstraede 101, Aalborg, DK-9220 Denmark
ars@et.aau.dk[1], yoy@et.aau.dk[2], fbl@et.aau.dk[3]

Abstract—In the case of a wide-scale adoption of grid-connected Photovoltaic (PV) systems, more fluctuated power will be injected into the grid due to the intermittency of solar PV energy. A sudden change in the PV power can potentially induce grid voltage fluctuations, and thus challenge the stability of the grid. Hence, this sudden active power change resulting in a large power ramp-rate should be avoided in practice. In fact, some grid regulations also released strict rules on active power ramp-rates for PV systems. This paper proposes a cost-effective control strategy to limit the power ramp-rate for two-stage grid-connected PV systems. The main concept of the proposed scheme is to modify the maximum power point tracking algorithm in such a way to regulate the PV power at the left side of the maximum power point curve. As a consequence, the power ramp-rate can be controlled according to the set-point. Experiments conducted on a 3-kW single-phase two-stage grid-connected PV system have verified that the proposed solution can accomplish fast dynamics, high accuracy, and high robustness in the power ramp-rate control for PV systems.

Index Terms—Active power control, ramp power control, maximum power point tracking, power curtailment, PV systems, grid-connected power converters.

I. Introduction

In recent years, the installation of grid-connected Photo-voltaic (PV) systems has been increasing with the aim to introduce more renewable energy into the mixed power grid [1]. As a consequence of the intermittent solar PV energy, a fluctuating power will continuously be injected into the grid. For instance, in some cases, the PV power may experience a sudden decrease or increase, e.g., due to passing clouds, which corresponds to large power ramp-rates. In fact, the changing rate of the PV power is also correlated with the size of the PV systems, as it has been studied in [2], [3]. A fast changing rate in the PV power is usually observed in residential/commercial PV systems with a small number of PV arrays, since a passing cloud can easily cover a major area of the PV plant. For example, a PV power change rate of 1 kW in 3 seconds was observed in a 2-kW PV systems during a cloudy day, as it was reported in [3]. In the case of a wide-scale grid-connected PV system, those sudden changes in the PV power can potentially induce severe grid voltage fluctuations [4], and thus being a challenging issue, especially for the stability of a
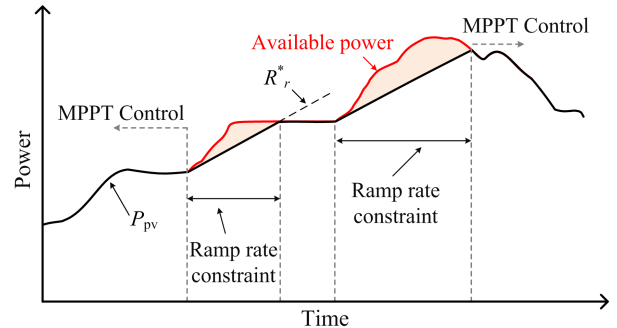

Fig. 1. Ramp-rate constraints defined in the Danish grid code, where P_{pv} is the PV output power and R_r^* is the reference ramp-rate limit [8].

weak distribution grid [5], [6]. Due to this, Power Ramp-Rate Control (PRRC) is introduced to limit the PV output power change rate [7], and it has been defined in the grid codes in some countries, e.g., Denmark [8] and the European Network of Transmission System Operators for Electricity (ENTSO-E) [9], which is illustrated in Fig. 1. Similar requirements are also stated in the grid code of Germany [10] and Puerto Rico [11], where a maximum ramp-rate of 10% of the rated PV power per minute is allowed.

Several methods to control the power ramp-rate of the PV output power have been reported in literature [12]–[22]. Integrating the energy storage systems is one of the most intuitive and commonly-used solutions [13]–[20], where the excessive energy from the PV can be stored in the storage device (e.g., battery, super capacitor) and thereby the power ramp-rate can be controlled. However, the energy storage systems will increase the cost and the size of the overall system. Besides, the limited lifetime of the energy storage device will also affect the lifetime of the overall PV systems, making this solution not very economically attractive [23]. Another way to control the power ramp-rate is achieved by disconnecting some of the PV panels in order to reduce the power production for a desired power ramp-rate. Nevertheless, this solution may not be feasible in the residential applications with a limited number of panels (e.g., rooftop PV systems). Moreover, a
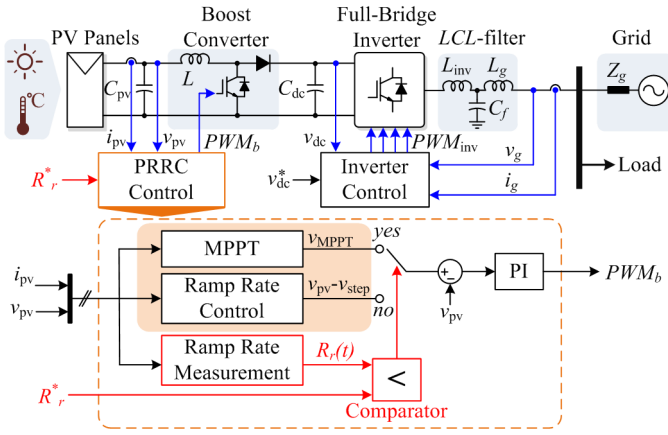
Fig. 2. System configuration and control structure of a two-stage single-phase grid-connected PV system with a Perturb and Observe based Power Ramp-Rate Control strategy (P&O-PRRC).

Rated PV power	3 kW
Boost converter inductor	L = 1.8 mH
PV-side capacitor	C_{pv} = 1000 μF
DC-link capacitor	C_{dc} = 1100 μF
LCL-filter	L_{inv} = 4.8 mH, L_g = 4 mH, C_f = 4.3 μF
Switching frequency	Boost converter: f_b = 16 kHz, Full-Bridge inverter: f_{inv} = 8 kHz
DC-link voltage	v_{dc}^* = 450 V
Grid nominal voltage (RMS)	V_g = 230 V
Grid nominal frequency	ω_0 = 2$\pi \times$50 rad/s

central control unit with a communication network to all PV inverters is also required, increasing both the system-level cost and complexity.

Actually, the power ramp-rate control can be realized through the active power curtailment by modifying the inherent MPPT algorithm at the PV inverter level [20], which is required for PV systems in normal operation mode. In this approach, no extra components are required and being a cost-effective solution. For instance in [21] a power ramp-rate control by modifying the MPPT algorithm is proposed, where the operating voltage of the PV system is obtained from the gradient-descent optimization algorithm. However, the limitations of this method are the out power fluctuation, which may occur during to the searching process, and the computation burden due to the optimization process. Another power ramp-rate control based on the modified MPPT algorithm is proposed in [22], where the power ramp-rate can be reduced by reversing the perturbation direction of a Perturb and Observe (P&O) MPPT algorithm. However, this method may lose its effectiveness in the case of fast dynamics (i.e., the changing irradiance), where the perturbation direction of the P&O MPPT always changes (the P&O MPPT algorithm can easily be confused by the change in the irradiance [24]). Therefore, reversing the perturbation direction cannot ensure an accurate power ramp-rate control for the PV system. Specifically, the algorithm in [22] can only control the power ramp-rate of the PV power under constant irradiance conditions.

Thus, this paper proposes a P&O-based Power Ramp-Rate Control (P&O-PRRC) strategy by modifying the MPPT algorithm to regulate the PV power at the left side of the Maximum Power Point (MPP) in the Power-Voltage (P-V) characteristic curve of the PV arrays, when the PRRC strategy is activated. In contrast to the method in [21], [22], the proposed solution can control the power ramp-rate of the PV system regardless of the irradiance conditions, and at the same time ensure a smooth and stable operational mode transitions. The implementation is also simple, as it will be discussed later on.

This paper is organized as follows: the P&O based Power Ramp-Rate Control (P&O-PRRC) strategy is discussed in Section II, where the system description and the control algorithm are presented. This includes a Ramp-Rate Measurement (RRM) and a Ramp-Rate Control (RRC), which are the two main components in the proposed solution. Then, the experimental validation of the P&O-PRRC strategy on a 3-kW single-phase two-stage PV system is carried out in Section III. The experimental results have confirmed the effectiveness of the proposal in terms of fast dynamics, high accuracy, and high robustness for power ramp-rate control. Finally, the conclusion is given in Section IV.

II. PROPOSED PERTURB AND OBSERVE BASED POWER RAMP-RATE CONTROL (P&O-PRRC) STRATEGY

A. System Description

Fig. 2 shows the overall system and control structure of a single-phase two-stage grid-connected PV system with its parameters being given in Table I. Here, a two-stage configuration is adopted, since it offers a wide range of MPPT operation [25], where the PV voltage v_{pv} can be stepped up by the boost converter to match the minimum dc-link voltage v_{dc}. In fact, this configuration is widely used in residential/commercial PV systems (e.g., with the rated power of 1-30 kW) [26], [27]. The boost converter is responsible for the PV power extraction, where the MPPT and/or PRRC algorithms are implemented in the control of the boost stage. Then, a full-bridge inverter delivers the extracted PV power to the ac grid, where the dc-link voltage v_{dc} is normally controlled as constant (e.g., 450 V) [28]. It also provides a proper synchronization between the PV side and the ac grid and, at the same time, ensures satisfied power quality of the injected grid current (e.g., the total harmonic distortion) with the phase-locked loop and the current controller implemented.

As aforementioned, modifying the MPPT algorithm has been found as a cost-effective solution to achieve the PRRC. The proposed P&O-based PRRC strategy consists of two main parts - Ramp-Rate Measurement (RRM) and Ramp-Rate Control (RRC), which will be discussed in the following.

B. Ramp-Rate Measurement (RRM)

It is important to have a fast and accurate ramp-rate measurement of the PV power in order to ensure the control performance. Usually, the PV power oscillates due to the MPPT algorithm (e.g., the P&O MPPT), which optimally should be within three operating points around the MPP [24], [29]. This implies that the changing rate of the PV power ΔP_{pv} is not zero even in the steady-state operation. Most of the prior-art solutions are thus using a moving average to filter out the power oscillations, and then the ramp-rate measurement can be accomplished [12]–[14]. This method is commonly used when the energy storage systems are employed for controlling the ramp-rate, and the purpose of the filtering is to avoid too often charging and discharging of the energy storage devices. However, the moving average method can deviate the ramp-rate calculation, and thus the estimation of the ramp-rate is slowed down [19]. Hence, it is not suitable for the P&O-PRRC strategy that requires fast dynamics.

A straightforward way to estimate the ramp-rate is enabled by measuring the PV power difference ΔP_{pv} in a certain period T_{RRM} as [17]

$$R_r(t) = \frac{dP_{pv}}{dt} = \frac{\Delta P_{pv}}{T_{RRM}} \tag{1}$$

$$= \frac{P_{pv}(t) - P_{pv}(t + T_{RRM})}{T_{RRM}} \tag{2}$$

$$= \frac{P_{pv}(t) - P_{pv}(t + nT_s)}{nT_s} \tag{3}$$

where $R_r(t)$ is the ramp-rate, $P_{pv}(t)$ is the measured PV power, n is an integer, T_s and T_{RRM} are the sampling periods of the MPPT and the RRM, respectively. If n is designed properly, the ramp-rate $R_r(t)$ will reflect the power changes induced by the solar irradiance instead of inherently by a MPPT control. Although this method is very simple, it should be pointed out that a large value of n will slow down the RRM. Moreover, the RRM is also dependent on the designed MPPT sampling frequency. An example of the RRM parameters selection is given in Fig. 3. Here the PV power with a ramp rate of 0.6 kW/s is used in the simulation, as it is shown in Fig. 3(a). Two different cases of RRM with $n = 20$ and $n = 50$ are shown in Figs. 3(b) and (c), respectively. In general, the simulation results agree with the previous discussion that a large value of n can reduce the variation in the ramp-rate (which is introduced by the inherent MPPT control and measurements), but it can also introduce significant delays in the RRM, as it is illustrated in Fig. 3(c).

C. Ramp-Rate Control (RRC)

Once the estimated ramp-rate $R_r(t)$ exceeds the ramp-rate limit R_r^*, the RRC algorithm will act in such a way that the output power of the PV is controlled accordingly. Eventually, the PV power changing rate will be within the limit (i.e., $R_r(t) = R_r^*(t)$). One way to reduce the PV power P_{pv} is by perturbing the operating point of the PV system away from the MPP in the Power-Voltage (P-V) characteristic curve of the PV arrays. In a two-stage PV system configuration, it is actually
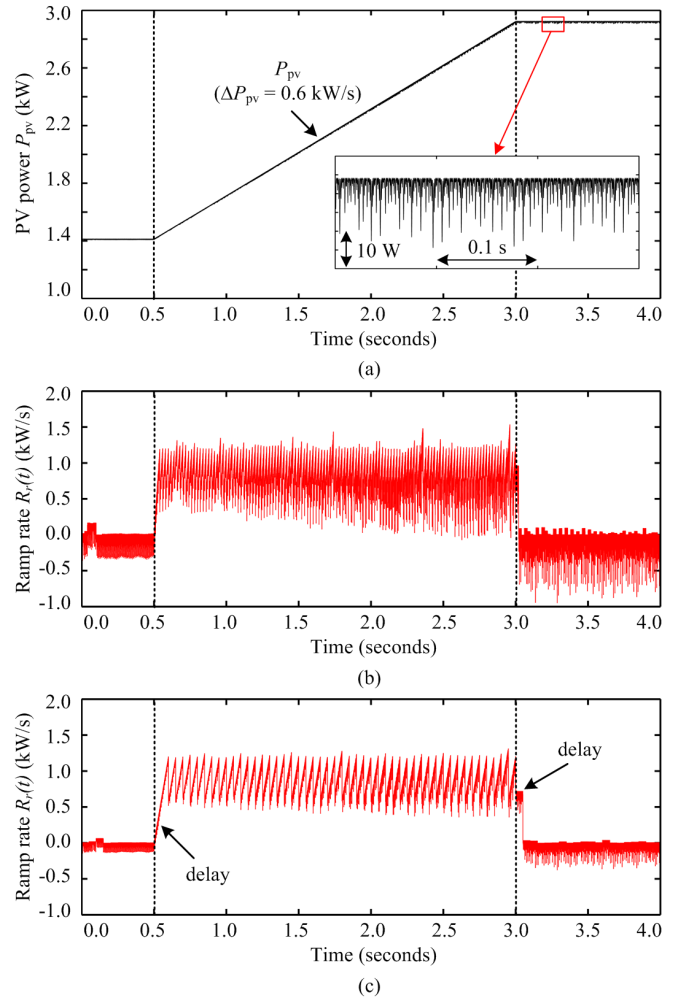

Fig. 3. Example of the ramp-rate measurement parameters selection: (a) PV power P_{pv}, (b) estimated ramp-rate $R_r(t)$ when $n = 20$, and (c) estimated ramp-rate $R_r(t)$ when $n = 50$.

possible to regulate the operating point of the PV system at either the left side (i.e., at A in Fig. 4) or the right side (i.e., at C in Fig. 4) of the MPP for a certain power ramp-rate, when the irradiance level increases (e.g., from 200 to 1000 W/m²), as it is illustrated in Fig. 4. However, it has been demonstrated in [30] that the operating region at the right side of the MPP can induce instability during a fast decreasing irradiance (e.g., from 1000 to 200 W/m² in Fig. 4 due to passing clouds), where the operating point of the PV system may fall into (and stay at) the open-circuit condition due to the decreased open-circuit voltage of the PV arrays V_{OC} (i.e., C→D in Fig. 4). Under this condition, the PV system will not be able to deliver any output power. In contrast, the operating region at the left side of the MPP can ensure a stable operation during a sudden irradiance drop, where it can be seen from the operating trajectory in Fig. 4 (i.e., A→B) that the operating point of the PV system will not go into open-circuit condition. Thus, for the stability concerns, the RRC algorithm regulates the PV power at the left side of the MPP (i.e., at A in Fig. 4).
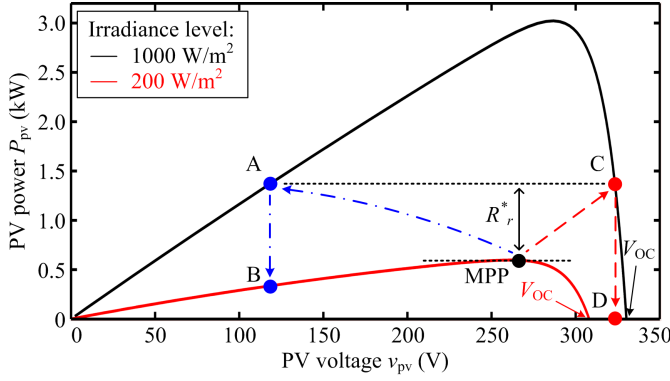
Fig. 4. Possible operating regions for the ramp-rate control algorithm, where the PV power P_{pv} can be regulated at the left side of the MPP or at the right side of the MPP for a certain ramp-rate R_r^*.
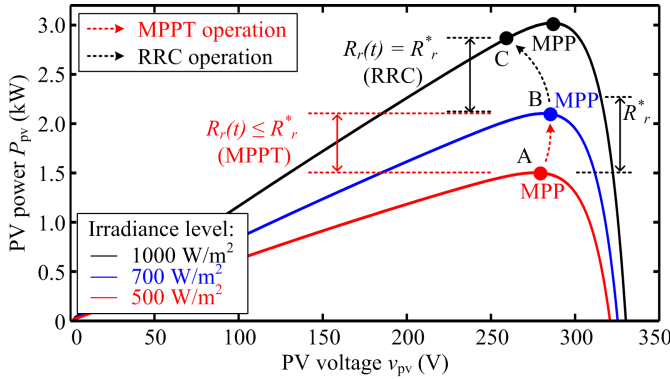

Fig. 5. Operational principle of the Power Ramp-Rate Control algorithm based on the Perturb and Observe method (P&O-PRRC).
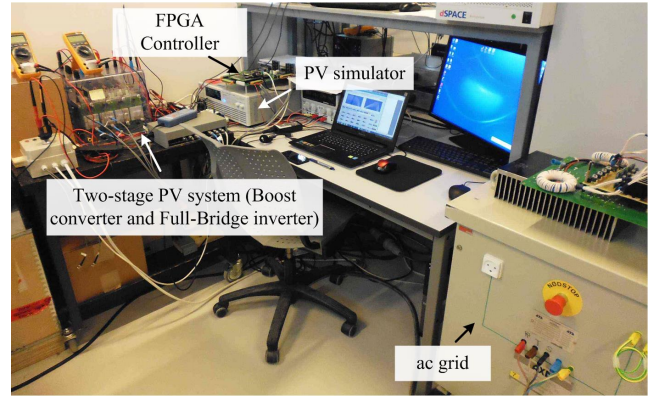

Fig. 6. Experimental setup of the two-stage grid-connected PV system.
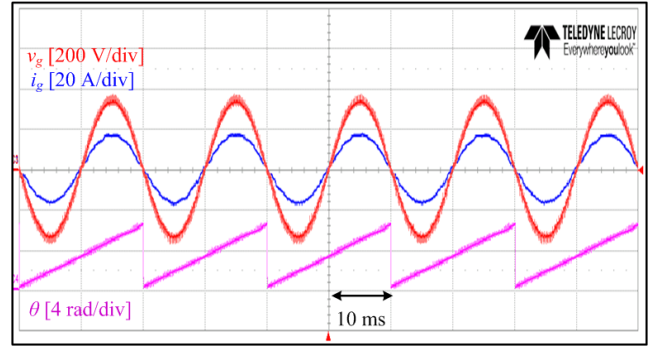

Fig. 7. Performance of the two-stage single-phase grid-connected PV system: (a) the PV power extraction during the MPPT operation, and (b) the grid voltage v_g, grid current i_g and the phase angle θ during the steady-state MPPT operation (3 kW).

Fig. 5 illustrates the operational principle of the RRC algorithm (i.e., operational mode transitions) during increasing irradiance condition. As long as the estimated ramp-rate $R_r(t)$ of (3) is below the reference limit R_r^* (e.g., when the irradiance level increases from 500 to 700 W/m^2), the PV system will keep operating in the MPPT operation (i.e., A→B in Fig. 5). During this period, the MPPT algorithm (i.e., the P&O MPPT) sets the voltage reference $v_{pv}^* = v_{MPPT}$ to control the boost converter, as it is shown in Fig. 2. Whilst, if $R_r(t) > R_r^*$ (e.g., when the irradiance level increases from 700 to 1000 W/m^2), the PV voltage v_{pv} will be continuously perturbed to the left side of the MPP (i.e., B→C in Fig. 5) in order to reduce the power ramp-rate. The RRC algorithm is summarized as

$$v_{pv}^* = \begin{cases} v_{MPPT}, & \text{when} \quad R_r(t) \leq R_r^* \\ v_{pv} - v_{step}, & \text{when} \quad R_r(t) > R_r^* \end{cases} \quad (4)$$

with v_{MPPT} being the reference voltage from the MPPT algorithm (e.g., P&O MPPT) and v_{step} is the perturbation step-size in order to achieve the RRC.

III. EXPERIMENTAL VALIDATION OF THE PROPOSED P&O-PRRC STRATEGY

In order to validate the performance of the proposed power ramp-rate control strategy (i.e., P&O-PRRC), experimental results have been carried out referring to Fig. 2. The system parameters are given in Table I. A PV simulator has been adopted with several irradiance profiles in order to emulate the power ramp-rate changes. The sampling frequencies of the MPPT and RRC algorithms are chosen to be 10 Hz (which is a typical sampling rate of the MPPT algorithm [24], [29]) while the sampling frequency of the RRM is designed as 0.4 Hz (i.e., $n = 25$, $T_s = 0.1$ s, $T_{RRM} = 2.5$ s according to (3)). The experimental test-rig is presented in Fig. 6, and Fig. 7 shows the performances of the single-phase grid-connected PV inverter system, where it can be seen that the grid voltage v_g and the phase angle θ are properly synchronized, and the injected current quality is satisfactory. The PV system operates also at a unity power factor where the grid voltage v_g is in phase with the grid current i_g, meaning that only the active power is injected into the grid. In the following, the proposed power ramp-rate control scheme is tested.

Firstly, two trapezoidal solar irradiance profiles are used to emulate a slow change and a fast change in the solar irradiance, respectively. The performance of the 3-kW PV system with the proposed P&O-PRRC strategy is presented in Fig. 8, where two ramp-rate limits R_r^* of 10 W/s and 20 W/s are adopted. Under a slow changing irradiance condition, the ramp-rate can accurately be controlled, as it can be seen
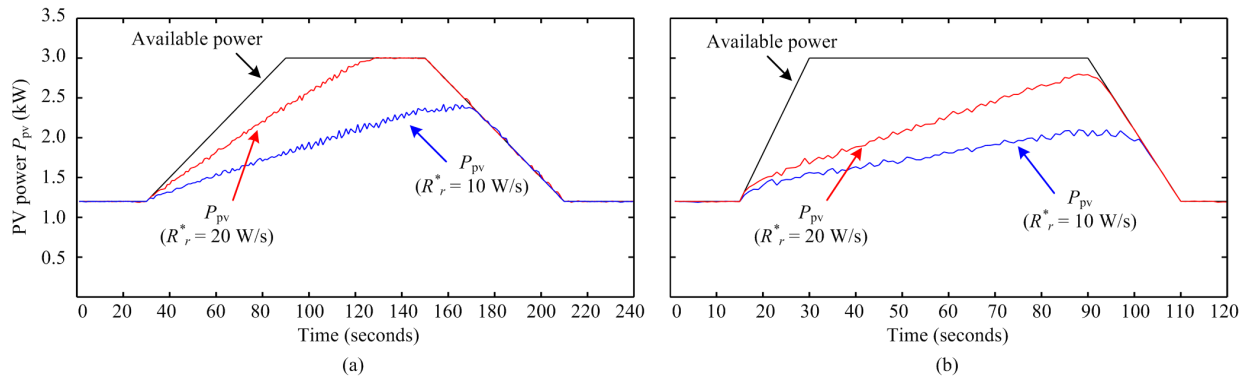
Fig. 8. PV output power (experiments) with the proposed PRRC strategy under: (a) a slow changing and (b) a fast changing irradiance conditions.
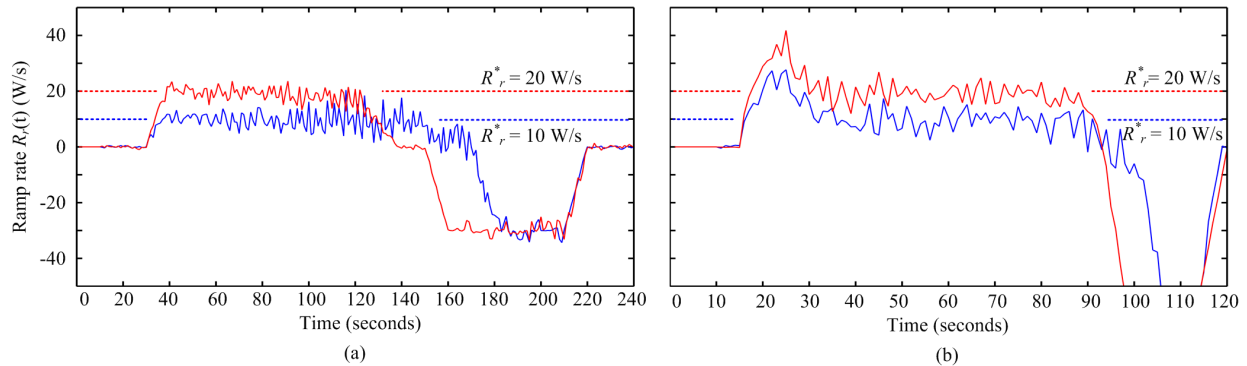

Fig. 9. Estimated instantaneous power ramp-rate of the proposed PRRC strategy under: (a) a slow changing and (b) a fast changing irradiance conditions.

from the estimated instantaneous ramp-rate of the PV power in Fig. 9(a). However, it is also observed in Fig. 9(b) that the instantaneous power ramp-rate $R_r(t)$ exceeds the limit when the irradiance level changes rapidly (e.g., in a cloudy day). Nevertheless, it only occurs in a short time period during transients, as demonstrated in Fig. 9(b). The performance of the P&O-PRRC algorithm is further examined with two real-field daily solar irradiance and ambient temperature profiles as shown in Fig. 10. In this case, an accelerated test (i.e., 60 times faster than the real profiles) has been performed, with the purpose to challenge the control algorithm in fluctuating irradiance conditions, and the ramp-rate is limited to 10 W/s. (One may notice that this ramp-rate of 10 W/s corresponds to 20%/minute, which exceeds the maximum limit in some grid codes, e.g., 10%/minute in Germany. However, the accelerate factor of the irradiance profile (i.e., 60 times faster) should be taken into consideration as well, when calculating the corresponding ramp-rate. In this case, the power ramp-rate of 20%/minute in the test can be considered to be equivalent to (20/60)%/minute = 0.33%/minute in reality). Fig. 11 shows the estimated instantaneous power ramp-rate, where it can be seen that the power ramp-rate $R_r(t)$ can be limited according to the reference in most cases. The ramp-rate limit is violated only during very fast transients, where the RRC algorithm requires a number of iterations to reduce P_{pv}. The experimental results have confirmed the effectiveness of the proposed power ramp-

rate control solution in terms of fast dynamics, high accuracy and high robustness for grid-connected PV system.

IV. CONCLUSION

A power ramp-rate control strategy for two-stage grid-connected PV systems has been proposed in this paper. The proposed method is achieved by modifying a conventional MPPT algorithm to regulate the operating point of the PV system to the left side of the maximum power point, and thus reduce the PV output power once the power ramp-rate exceeds the reference set-point. In this way, the power ramp-rate of the PV power can be limited in practice without extra component requirements, being a cost-effective solution compared to the prior-art solutions. Experimental results have validated the effectiveness of the power ramp-rate control method in terms of fast dynamics, high accuracy and high robustness.
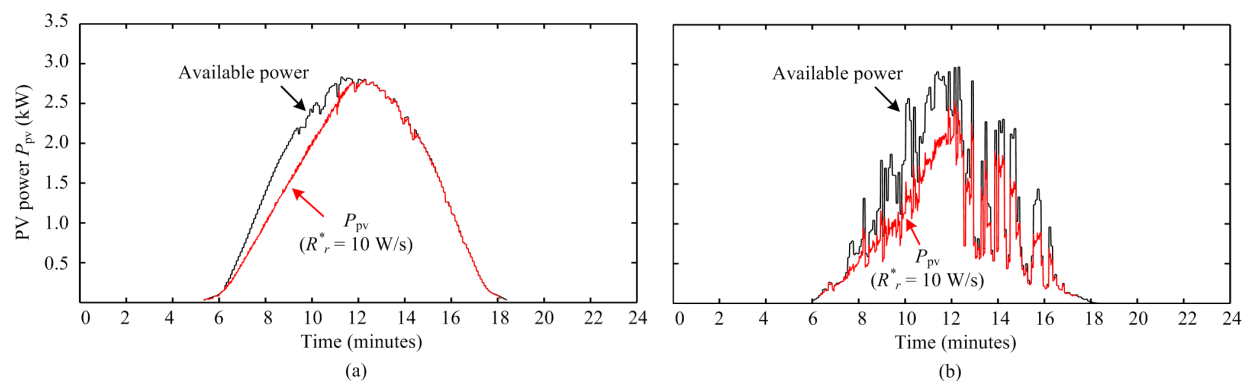
Fig. 10. PV output power (experiments) with the proposed PRRC control strategy under: (a) a clear day and (b) a cloudy day irradiance conditions.
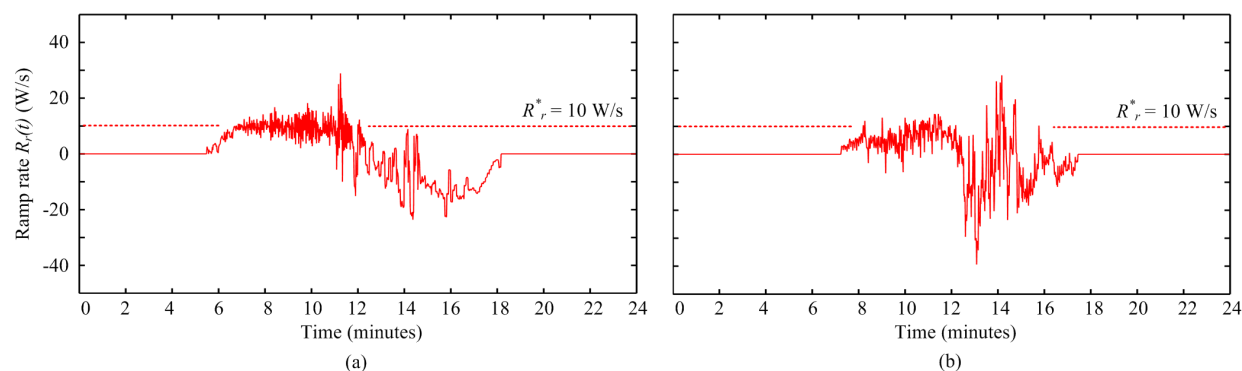

Fig. 11. Estimated instantaneous power ramp-rate of the proposed PRRC strategy under: (a) a clear day and (b) a cloudy day irradiance conditions.

REFERENCES

[1] Solar Power Europe, "Global Market Outlook For Solar Power 2015 - 2019," 2015. [Online]. Available: http://www.solarpowereurope.org/.

[2] M. K. Hossain and M. H. Ali, "Statistical analysis of ramp rates of solar photovoltaic system connected to grid," in *Proc. of ECCE*, pp. 2524–2531, Sep. 2014.

[3] D. Cormode, A. D. Cronin, W. Richardson, A. T. Lorenzo, A. E. Brooks, and D. N. DellaGiustina, "Comparing ramp rates from large and small PV systems, and selection of batteries for ramp rate control," in *Proc. of PVSC*, pp. 1805–1810, June 2013.

[4] A. Woyte, V. V. Thong, R. Belmans, and J. Nijs, "Voltage fluctuations on distribution level introduced by photovoltaic systems," *IEEE Trans. on Energy Convers.*, vol. 21, no. 1, pp. 202–209, Mar. 2006.

[5] Y. Yang, P. Enjeti, F. Blaabjerg, and H. Wang, "Wide-scale adoption of photovoltaic energy: Grid code modifications are explored in the distribution grid," *IEEE Ind. Appl. Mag.*, vol. 21, no. 5, pp. 21–31, Sep. 2015.

[6] M. Karimi, H. Mokhlis, K. Naidu, S. Uddin, and A. Bakar, "Photovoltaic penetration issues and impacts in distribution network - a review," *Renewable and Sustainable Energy Reviews*, vol. 53, pp. 594 – 605, 2016.

[7] National Renewable Energy Laboratory, "Industry perspectives on advanced inverters for U.S. solar photovoltaic systems: Grid benefits, deployment challenges, and emerging solutions," Tech. Rep., 2015.

[8] Energinet.dk, "Technical regulation 3.2.2 for PV power plants with a power output above 11 kW," Tech. Rep., 2015.

[9] European Network of Transmission System Operators for Electricity, "Network code for requirements for grid connection applicable to all generators," Tech. Rep., Mar. 2013. [Online]. Available: https://www.entsoe.eu.2013

[10] BDEW, "Technische richtlinie erzeugungsanlagen am mittelspannungsnetz richtlinie fur anschluss und parallelbetrieb von erzeugungsanlagen am mittelspannungsnetz," Jun. 2008.

[11] National Renewable Energy Laboratory, "Reviewe of PREPA technical requirements for interconnecting wind and solar generation," Tech. Rep., 2013.

[12] S. Shivashankar, S. Mekhilef, H. Mokhlis, and M. Karimi, "Mitigating methods of power fluctuation of photovoltaic (PV) sources - a review," *Renewable and Sustainable Energy Reviews*, vol. 59, pp. 1170 – 1184, 2016.

[13] N. Kakimoto, H. Satoh, S. Takayama, and K. Nakamura, "Ramp-rate control of photovoltaic generator with electric double-layer capacitor," *IEEE Trans. on Energy Convers.*, vol. 24, no. 2, pp. 465–473, June 2009.

[14] R. van Haaren, M. Morjaria, and V. Fthenakis, "An energy storage algorithm for ramp rate control of utility scale PV (photovoltaics) plants," *Energy*, vol. 91, pp. 894 – 902, 2015.

[15] X. Li, D. Hui, and X. Lai, "Battery energy storage station (BESS)-based smoothing control of photovoltaic (PV) and wind power generation fluctuations," *IEEE Trans. on Sustain. Energy*, vol. 4, no. 2, pp. 464–473, Apr. 2013.

[16] M. Chamana, F. Jahanbakhsh, B. H. Chowdhury, and B. Parkhideh, "Dynamic ramp rate control for voltage regulation in distribution systems with high penetration photovoltaic power generations," in *Proc. of IEEE Power Energy Soc. General Meet.*, pp. 1–5, July 2014.

[17] V. Salehi and B. Radibratovic, "Ramp rate control of photovoltaic power plant output using energy storage devices," in *Proc. of IEEE Power Energy Soc. General Meet.*, pp. 1–5, July 2014.

[18] J. Marcos, O. Storkel, L. Marroyo, M. Garcia, and E. Lorenzo, "Storage requirements for PV power ramp-rate control," *Solar Energy*, vol. 99, pp. 28–35, 2014.

[19] M. J. E. Alam, K. M. Muttaqi, and D. Sutanto, "A novel approach for ramp-rate control of solar PV using energy storage to mitigate output fluctuations caused by cloud passing," *IEEE Trans. on Energy Convers.*, vol. 29, no. 2, pp. 507–518, June 2014.

[20] W. A. Omran, M. Kazerani, and M. M. A. Salama, "Investigation of methods for reduction of power fluctuations generated from large grid-connected photovoltaic systems," *IEEE Trans. on Energy Convers.*, vol. 26, no. 1, pp. 318–327, Mar. 2011.

[21] N. Ina, S. Yanagawa, T. Kato, and Y. Suzuoki, "Smoothing of PV system output by tuning mppt control," *Electrical Engineering in Japan*, vol. 152, no. 2, pp. 10–17, 2005.

[22] R. Yan and T. K. Saha, "Power ramp rate control for grid connected photovoltaic system," in *Proc. of IPEC*, pp. 83–88, Oct. 2010.

[23] S. Bacha, D. Picault, B. Burger, I. Etxeberria-Otadui, and J. Martins, "Photovoltaics in microgrids: An overview of grid integration and energy management aspects," *IEEE Ind. Electron. Mag.*, vol. 9, no. 1, pp. 33–46, Mar. 2015.

[24] N. Femia, G. Petrone, G. Spagnuolo, and M. Vitelli, "Optimization of perturb and observe maximum power point tracking method," *IEEE Trans. on Power Electron.*, vol. 20, no. 4, pp. 963–973, July 2005.

[25] H. Ghoddami and A. Yazdani, "A bipolar two-stage photovoltaic system based on three-level neutral-point clamped converter," in *Proc. of IEEE Power Energy Soc. Gen. Meet*, pp. 1–8, Jul. 2012.

[26] S.B. Kjaer, J.K. Pedersen, and F. Blaabjerg, "A review of single-phase grid-connected inverters for photovoltaic modules," *IEEE Trans. Ind. Appl.*, vol. 41, no. 5, pp. 1292–1306, Sep. 2005.

[27] SMA, "Medium power solutions," Sunny family 2011/2012, Tech. Rep.

[28] F. Blaabjerg, R. Teodorescu, M. Liserre, and A.V. Timbus, "Overview of control and grid synchronization for distributed power generation systems," *IEEE Trans. Ind. Electron.*, vol. 53, no. 5, pp. 1398–1409, Oct. 2006.

[29] M. Elgendy, B. Zahawi, and D. Atkinson, "Assessment of perturb and observe mppt algorithm implementation techniques for PV pumping applications," *IEEE Trans. on Sustain. Energy*, vol. 3, no. 1, pp. 21–33, Jan. 2012.

[30] A. Sangwongwanich, Y. Yang, F. Blaabjerg, and H. Wang, "Benchmarking of constant power generation strategies for single-phase grid-connected photovoltaic systems," in *Proc. of APEC*, pp. 370–377, Mar. 2016.